Detecting the dominant contributions of runoff variance across the source region of the Yellow River using a new decomposition framework

Jingkai Xie, Yue-Ping Xu, Yuxue Guo and Yitong Wang

ABSTRACT

Quantifying the contributions of climatic variables to runoff variance is still a great challenge to water resource management. This study adopted an extended Budyko framework to investigate the effects of terrestrial water storage changes (ΔS) on runoff variance across the source region of the Yellow River, China, during the period of 2003–2014. A new decomposition framework based on the extended Budyko framework was proposed to effectively quantify the contributions of different climatic variables including precipitation, *PET* and ΔS to runoff variance. The results demonstrated that the extended Budyko framework showed a better performance in presenting the water and energy balance than the original Budyko framework, especially at fine time scales. Meanwhile, the variance in runoff estimated by the new decomposition framework was close to that of runoff observations, indicating that this framework can effectively capture the variation in runoff during 2003–2014. It was also found that precipitation was the most important factor that contributed to runoff changes, while *PET* made a slightly smaller contribution compared to precipitation. Notably, the results also emphasized the important effects of ΔS on runoff variance at fine time scales, which was useful to better understand the interactions between atmospheric and hydrological processes for regions.

Key words | climatic variability, extended Budyko framework, runoff, source region of the Yellow River, terrestrial water storage changes, water balance

HIGHLIGHTS

- A new decomposition framework was proposed to effectively quantify the contributions of different climatic variables to runoff variance.
- Precipitation was the most important factor that contributed to runoff changes, while *PET* made a slightly smaller contribution compared to precipitation.
- The important effects of ΔS on runoff variance at fine time scales can not be neglected.

Jingkai Xie
Yue-Ping Xu (corresponding author)
Yuxue Guo
Yitong Wang
Institute of Hydrology and Water Resources, Civil Engineering,
Zhejiang University,
Hangzhou 310058,
China
E-mail: *yuepingxu@zju.edu.cn*

doi: 10.2166/nh.2021.179

INTRODUCTION

Runoff is an important source of natural freshwater resources, which has been regarded as the fundamental element in social and economic development (Tikhamarine *et al.* 2020). Understanding the main drivers of runoff changes and variability is essential to decision-making in regional freshwater resource planning and management (Berghuijs *et al.* 2017). During the past decades, impacts of climatic variability on runoff magnitude have attracted widespread attention from many hydrologists and water resource managers. It is reported that about 31% of 145 major rivers across the world have shown significant changes in the mean annual runoff during the past decades (Walling & Fang 2003; Zhai & Tao 2017). Therefore, a comprehensive and quantitative understanding of runoff variance and its main sources is totally necessary for the evaluation of hydrological models (Wang & Hejazi 2011), climatic variability impact assessment (Collins *et al.* 2013) and uncertainty quantification in runoff estimation (Bock *et al.* 2018).

Numerous attribution methodologies have been proposed to separate the individual impact of climatic variability on runoff including hydrological modeling (Darvini & Memmola 2020), hydrological sensitivity method (Zuo *et al.* 2014) and climate elasticity method (Dey & Mishra 2017). For example, Ma *et al.* (2010) conducted a quantitative assessment of the influence of climatic variability on runoff reduction in the Miyun Reservoir basin, in China, by jointly using a distributed hydrological model and a climate elasticity model. Li *et al.* (2020) partitioned the contributions of precipitation and glacier melt to the runoff in a headwater basin of the Tarim River using a glacio-hydrological model and found that both rainfall and glacier melt are the primary causes of increased runoff in the study area during the period of 1971–2010. Chiew *et al.* (2006) estimated the sensitivity of runoff to the mean annual precipitation across the world based on an elasticity indicator and concluded that annual changes in precipitation were amplified in runoff, that is, a 1% change in the mean annual precipitation resulted in a 1–3% change in the mean annual streamflow globally.

Aside from various attribution methodologies mentioned above, the water balance method in combination with the Budyko framework has been considered as another useful approach to assess the contributions of different climatic variables and basin characteristics to runoff changes. The Budyko framework has been widely used in previous studies because it can accurately reflect the balance between water availability and energy supply across the study regions (Liang *et al.* 2014; Chen *et al.* 2020; Yang *et al.* 2020). Zhou *et al.* (2016) proposed a new partition method to distinguish the climate and basin attributes on the mean annual runoff within the Budyko complementary relationship. Zhang *et al.* (2019) conducted a Budyko-based framework with the purpose of quantifying the impacts of aridity index and other factors on annual runoff in 355 catchments selected from the United States. Notwithstanding that many attempts have been made to reveal the mechanism about how climatic variables influence runoff, there still exist some limitations in these studies. For example, the effect of changes in terrestrial water storage, which is an important component of the hydrological cycles for regions (Xie *et al.* 2019b), on runoff variance, is unknown because it has long been neglected when applying the Budyko framework to assess the effects of climatic variability on runoff. In addition, a quantitative analysis of variations in runoff at fine time scales (i.e. season or month) is also rarely made.

The source region of the Yellow River (hereafter SRYR), supplying water for millions of people, is an important region in China. Identifying and analyzing the variations in runoff across the SRYR is useful not only for understanding the water and energy balance between atmospheric and land surface hydrologic processes but also for improving the water resource management across the entire Yellow River basin (Xu *et al.* 2018). In addition, the mechanism behind runoff changes in the SRYR has attracted intensive concern in the decade owing to its link to the 'Three Rivers Source Region Reserve' and 'Grain for Green Project'. Several studies have shown that the SRYR has experienced a significant decrease in runoff in recent years (Wang *et al.* 2018; Chu *et al.* 2019), which will further lead to variations in the temporal and spatial distributions of the water resources in the whole Yellow River basin. However, it has long been challenging to accurately assess the contributions of various natural

drivers to runoff variance for this region due to its harsh environment and complex topography. Therefore, it is necessary and meaningful to quantify the contributions of various climatic variables to runoff, which will not only provide valuable guidance for decision-makers in making appropriate policies for water resource assessment but can also help hydrologists better understand runoff response to climatic variability.

As mentioned above, enough knowledge of the temporal variability of runoff is imperative to a comprehensive understanding of hydrological processes under climatic variability. Although previous studies have consistently investigated the effects of climatic variability on runoff to some extent, they fail to accurately quantify the contributions of these factors to runoff variance (Zarghami *et al.* 2011; Li *et al.* 2013; Lei *et al.* 2014). The main objective of this study is, therefore, to investigate the applicability of the extended Budyko framework by incorporating the effects of terrestrial water storage changes (hereafter ΔS) on regional water and energy balance at different time scales. Meanwhile, a new variance decomposition framework is developed to quantify the main factors influencing the runoff for the SRYR at intra-annual and inter-annual time scales, respectively. To our knowledge, current studies about the impacts of ΔS and other factors on runoff variance at fine time scales are still rare. Therefore, this study will be beneficial for accurately quantifying the response of hydrological cycles to climatic variability, especially for regions with limited hydrological data.

The other parts of this paper are mainly structured as follows. In the 'Study area' section, the study area is briefly described. The 'Data' and 'Methods' sections present the data and methods used in this study, respectively. The 'Results' section contains all the results illustrating the water balances of basins based on the extended Budyko framework at different time scales. Meanwhile, the effects of different factors on variations in runoff are also included in this section. Finally, all the discussion and major conclusions are presented in the 'Discussion' and 'Conclusions' sections, respectively.

STUDY AREA

The SRYR mainly refers to the region controlled by the Tangnaihai (hereafter TNH) hydrological station located in the mainstream of the Yellow River, which is the second-longest river in China with a length of over 5,400 km (shown in Figure 1). The SRYR has a drainage area of 1.22×10^5 km^2 and accounts for approximately 15.2% of the area of the entire Yellow River basin. This region is situated in the northeastern Tibetan Plateau, which has an average altitude of over 4,000 meters above sea level. Due to its extremely harsh environment and climatic conditions, the SRYR has long been a sparsely populated region, and therefore this region can be viewed as a relatively pristine area with few human activities (Zheng *et al.* 2009). The SRYR, sometimes also termed as 'the cistern of the Yellow River', occupies only approximately 15.2% of the total area of the Yellow River basin but yields 35% of the total annual discharge of the Yellow River (Zheng *et al.* 2007; Yuan *et al.* 2018; Si *et al.* 2019). Therefore, the SRYR plays a considerable role in the downstream water resource management and hydrological cycles through the entire Yellow River basin.

The climate of the SRYR belongs to the typical Qinghai–Tibet Plateau climate system, which is characterized by distinct wet and dry seasons (Xu *et al.* 2018). Mainly influenced by the southwest monsoon from the Bay of Bengal, more than 70% of the annual precipitation across the SRYR occurs from June to September (Liang *et al.* 2010). For the period of 2003–2014, the mean annual precipitation of the SRYR is 583 mm while the annual *PET* is 837 mm, with an aridity index (*PET*/*P*) of 1.44. In addition, the annual runoff depth of the SRYR at the TNH hydrological station ranges from 109 to 220 mm with a mean value of 156 mm.

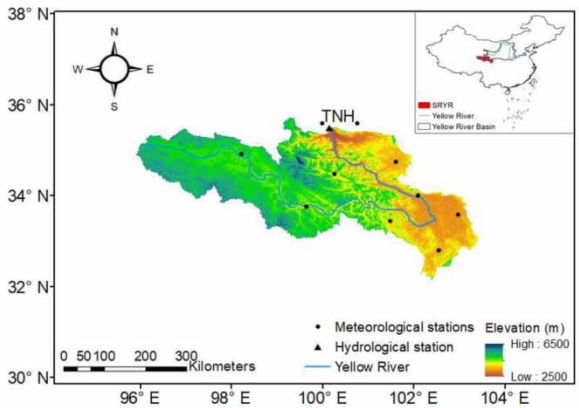

Figure 1 | Study region maps showing the distribution of meteorological stations and the hydrological station across the SRYR. TNH, Tangnaihai hydrological station.

Runoff coefficients range from 0.21 to 0.33 with an average of 0.27 during the same period mentioned above. More information about the related hydrological station, meteorological stations, geographical locations and drainage distribution of the SRYR have been depicted in Figure 1.

DATA

Evapotranspiration

Evapotranspiration (*ET*) is one of the most important elements in hydrological cycles, which can reflect the true state of water balance and energy exchanges in hydrological systems at different scales from field to global. However, *ET* has been extremely hard to measure or quantify through direct observations, especially in some regions with limited observations (Xing *et al.* 2018; Xie *et al.* 2019a). To estimate the variations in *ET* during the study period, three different datasets are jointly selected to estimate regional evapotranspiration in this study, namely (1) *ET* from the Global Land Data Assimilation System with Noah Land Surface Version 2 (hereafter ET_GLDAS, https://earthdata.nasa.gov/); (2) *ET* from Moderate Resolution Imaging Spectroradiometer (hereafter ET_MODIS, http://www.ntsg.umt.edu/project/mod16); and (3) *ET* from the Global Land Evaporation Amsterdam Model (hereafter ET_GLEAM, https://www.gleam.eu). Although these three *ET* products were derived from different principles or methods, all of them have been widely validated and applied in different regions including the SRYR because of their high quality and reliability (Xue *et al.* 2013; Liu *et al.* 2016; Ahlstrom *et al.* 2017; Asoka *et al.* 2017; Guo *et al.* 2017; Chang *et al.* 2018; Khan *et al.* 2018; Wang *et al.* 2018; Yang *et al.* 2021). In the following sections, the ensemble mean of these three independent *ET* products is used to describe the variations in actual *ET* across the study region.

Meteorological data and *in situ* runoff observations

Meteorological data, including daily observations of mean air temperature (T), sunshine duration (s), relative humidity (RH) and wind speed (u) for the period 2003–2014, are collected from China Meteorological Administration (CMA, http://data.cma.cn/). All the above data are jointly used to obtain daily time series of potential evapotranspiration (*PET*) across the study region. In addition, the Thiessen polygon method is adopted to estimate daily time series of precipitation (P) across the study region using observations from different meteorological stations (shown in Figure 1), which are further aggregated to monthly results.

From the Yellow River Conservancy Commission, daily time series of runoff (R) observations during 2003–2014 are obtained at the TNH gauging station, which has been selected as the outlet of the SRYR. Furthermore, daily values of runoff observations are aggregated to monthly results with the purpose of keeping consistent with other variables in the water balance equation.

GRACE-derived data

Terrestrial water storage mainly refers to all the forms of water stored under the earth (i.e. soil moisture and groundwater) and above the earth (i.e. lakes, rivers, wetlands and reservoirs). Variations in terrestrial water storage can reflect the budget between water input and water output for regions. The successful launch of the GRACE satellite has provided a new insight into the variations in terrestrial water storage, especially in some regions with few *in situ* observations (Song *et al.* 2015; Zhang *et al.* 2020). Since the GRACE satellite can effectively detect the variations in terrestrial water storage, in this study, three different GRACE mascon products are also jointly used to estimate ΔS with the purpose of validating the accuracy and reliability of results that are estimated by the water balance method. Note that some monthly values of GRACE data are missing because of 'battery management' during the study period. Therefore, these missing values are linearly interpolated from the previous and following months of the corresponding missing data. More detailed descriptions of datasets that are used in this study can be found in Table 1.

METHODS

Penman–Monteith method

In this study, daily time series of potential evapotranspiration are calculated based on the Penman–Monteith

Table 1 | Overview of datasets used in this study

Variables		Spatial resolution	Temporal resolution	Temporal extent	Data references
Evapotranspiration (*ET*)	GLDAS2.0 Noah	0.25°	Monthly	1948–2014	Rodell *et al.* (2004a)
	GLEAM	0.25°	Daily	2003–2017	Martens *et al.* (2017); Miralles *et al.* (2011)
	MODIS16	0.5°	Monthly	2000–2014	Mu *et al.* (2007)
Terrestrial water storage changes (ΔS)	GRACE-CSR Mascon	0.5°	Monthly	2002–2017	Save *et al.* (2016)
	GRACE-JPL Mascon	0.5°	Monthly	2002–2017	Landerer & Swenson (2012); Swenson & Wahr (2006)
	GRACE-GSFC Mascon	0.5°	Monthly	2002–2017	Awange *et al.* (2011); Luthcke *et al.* (2013)
Runoff (*R*)		–	Daily	2003–2014	–
Precipitation (*P*)		–	Daily	2003–2014	
Air temperature (*T*)		–	Daily	2003–2014	
Wind speed (*u*)		–	Daily	2003–2014	
Sunshine duration (*s*)		–	Daily	2003–2014	
Relative humidity (*RH*)		–	Daily	2003–2014	

equation, which is viewed as one of the most optimal methods to reflect the energy availability for regions (Leuning *et al.* 2008; Irmak & Mutiibwa 2010; Mcjannet *et al.* 2013; Mallick *et al.* 2015). The Penman–Monteith method is shown as follows:

$$PET = \frac{0.408\Delta(R_n - G) + \gamma\left(\frac{900}{(T+273)}\right)u(e_s - e_a)}{\Delta + \gamma(1 + 0.34u)} \quad (1)$$

where PET is the potential evapotranspiration (mm day^{-1}); Δ is the slope of the saturated vapor pressure–temperature curve (kPa $°C^{-1}$); R_n is net radiation at the canopy surface (MJ m^{-2} day^{-1}); G is the soil heat flux (MJ m^{-2} day^{-1}); γ is a psychrometric constant (kPa $°C^{-1}$); T is the mean air temperature at a height of 2 m (°C); u is the wind speed at a height of 2 m (m s^{-1}); e_s is the saturated vapor pressure at a height of 2 m; and e_a is the actual vapor pressure at a height of 2 m. Furthermore, daily time series of PET are aggregated to monthly PET with the purpose of maintaining consistency with ET and P.

Estimation and validation of terrestrial water storage change (ΔS)

The effects of ΔS on runoff variance have not been comprehensively examined before, mainly due to the lack of accurate observations of terrestrial water storage. To detect the changes in terrestrial water storage over the SRYR, the basin-scale water balance method is applied to estimate the monthly ΔS across the SRYR (Wan *et al.* 2015; Lv *et al.* 2017), which can be described as follows:

$$\Delta S = P - R - ET \quad (2)$$

where ΔS is terrestrial water storage changes (mm); P is precipitation (mm); R is runoff (mm); ET is evapotranspiration (mm), which can be estimated by the average of three different evapotranspiration products as mentioned in the 'Evapotranspiration' section.

Monthly time series of ΔS across the SRYR are obtained based on the water balance method (Equation (2)). To further validate the accuracy of these results derived from the water balance method, the changes in terrestrial water storage across the SRYR are also estimated based on

GRACE data independently:

$$\Delta S' = \frac{TWSA(m+1) - TWSA(m-1)}{2} \quad (3)$$

where $\Delta S'$ is GRACE-derived terrestrial water storage changes (mm); $TWSA(m+1)$ is terrestrial water storage anomalies (mm) for month $(m+1)$, while $TWSA(m-1)$ is terrestrial water storage anomalies (mm) for month $(m-1)$. Previous studies (Long *et al.* 2014; Xie *et al.* 2019a) have indicated that this method can not only be used effectively to estimate the regional ΔS but also includes some light numerical smoothing.

Original and extended Budyko frameworks

Budyko (1974) assumed that actual ET for regions can change under the joint effects of energy and water availabilities. Hence, the Budyko framework is reflecting water and energy balance for regions, which can be represented as Fu's equation (Fu 1981; Zhang *et al.* 2004):

$$\frac{\overline{ET}}{\bar{P}} = F(\bar{\varnothing}) = 1 + \frac{\overline{PET}}{\bar{P}} - \left[1 + \left(\frac{\overline{PET}}{\bar{P}}\right)^{\bar{n}}\right]^{\frac{1}{\bar{n}}} \quad (4)$$

where $\bar{\varnothing}\left(=\frac{\overline{PET}}{\bar{P}}\right)$ is the long-term average aridity index for study regions; P and PET are precipitation (mm) and potential evapotranspiration (mm), respectively; $\bar{n}$ is the parameter reflecting basin-specific characteristics, such as soil moisture, vegetation cover and climate seasonality (Yang *et al.* 2008; Zheng *et al.* 2018), which can be estimated by the least squares method.

Traditionally, the time scale when applying the Budyko framework has been defined as the long-term average (Patterson *et al.* 2013; Greve *et al.* 2020). In fact, recent studies have also made attempts to extend this equation with the purpose of validating the variability of annual or even monthly water balance in different regions (Yang *et al.* 2007; Zhang *et al.* 2008; Carmona *et al.* 2014). Therefore, Fu's equation at monthly or annual scales has been further modified as:

$$\frac{ET}{P} = F(\varnothing) = 1 + \frac{PET}{P} - \left[1 + \left(\frac{PET}{P}\right)^{n}\right]^{\frac{1}{n}} \quad (5)$$

where $\varnothing$ $(=PET/P)$ and n represent the aridity index and the basin characteristics parameter at different time scales such as annual or monthly.

Although it can capture the annual water energy and water balances for some river basins, the original Budyko framework will not work at finer time scales which has been demonstrated by several studies (Wang *et al.* 2009; Istanbulluoglu *et al.* 2012). Wang (2012) pointed out that the influences of ΔS should not be neglected anymore when applying the Budyko framework at annual or monthly scales for regions. That is to say, ΔS may play a more important role in determining hydrologic response at the intra-annual scales. To better describe the actual variability of water balance for regions under non-steady-state conditions, it is very necessary to take the influences of ΔS into consideration, which can be obtained from Equation (2). Chen *et al.* (2013) suggested replacing atmospheric water supply (P) by the total available water (P') in Equation (5), and therefore the original Budyko framework can be extended into:

$$\frac{ET}{P'} = F(\varnothing') = 1 + \frac{PET}{P'} - \left[1 + \left(\frac{PET}{P'}\right)^{n}\right]^{\frac{1}{n}} \quad (6)$$

where P' $(=P-\Delta S)$ is effective precipitation (mm), which represents the total available water for regions and mainly depends on both atmospheric water supply and basin storage (Wu *et al.* 2017a,); $\varnothing'$ $(=PET/P')$ represents the aridity index considering ΔS; and n is the basin characteristics parameter, which can be obtained based on the least squares method.

In this study, both Equations (5) and (6) are applied in the SRYR at the annual, seasonal and monthly timescales, respectively, with the purpose of investigating the effects of ΔS on water and energy balance across the SRYR at different time scales.

Runoff variance decomposition framework

To further quantify the effects of climatic factors (including P and PET) and basin storage changes (i.e. ΔS) on runoff, a new variance decomposition framework is proposed in this study. According to the water balance equation and assuming that the long-term storage change $\overline{\Delta S} = 0$, the observed

runoff (R) deviation from its long-term mean ($\bar{R}$) at a specific time interval can be expressed as follows:

$$\begin{aligned}\Delta R_i &= R_i - \bar{R} = (P_i - ET_i - \Delta S_i) - (\bar{P} - \overline{ET} - \overline{\Delta S}) \\ &= \Delta P_i - \Delta ET_i - \Delta S_i \end{aligned} \tag{7}$$

where ΔR_i, ΔP_i, ΔET_i and ΔS_i refer to the changes in runoff, precipitation, evapotranspiration and terrestrial water storage at a specific time interval, such as month, season or year.

As suggested by Zeng & Cai (2015), changes in ET (i.e. ΔET_i) for regions mainly consist of different changes in P, PET and ΔS, respectively, which can be described as:

$$\begin{aligned}\Delta ET_i =& \Delta P_i[F(\bar{\varnothing}) - F'(\bar{\varnothing})\bar{\varnothing}] - \Delta S_i[F(\bar{\varnothing}) - F'(\bar{\varnothing})\bar{\varnothing}] \\ &+ \Delta PET_i F'(\bar{\varnothing}) \end{aligned} \tag{8}$$

where ΔR_i, ΔP_i and ΔS_i are the same as that shown in Equation (7), ΔPET_i represents changes in potential evapotranspiration, $\bar{\varnothing}$ is the long-term average aridity index, $F(\bar{\varnothing})$ and $F'(\bar{\varnothing})$ are the Budyko framework and its first-order derivative, respectively.

To further substitute the term of ΔET_i from Equation (7) into Equation (8) yields:

$$\begin{aligned}\Delta R_i =& \Delta P_i[1 - F(\bar{\varnothing}) + F'(\bar{\varnothing})\bar{\varnothing}] - \Delta S_i[1 - F(\bar{\varnothing}) + F'(\bar{\varnothing})\bar{\varnothing}] \\ &- \Delta PET_i F'(\bar{\varnothing}) \end{aligned} \tag{9}$$

The sample variance of R can therefore be derived by taking the square of Equation (9), summing over N samples and scaled by $N-1$:

$$\begin{aligned}\sigma_R^2 =& w_P\sigma_P^2 + w_{PET}\sigma_{PET}^2 + w_{\Delta S}\sigma_{\Delta S}^2 + w_{P,PET}\mathrm{cov}(P, PET) \\ &+ w_{P,\Delta S}\mathrm{cov}(P, \Delta S) + w_{PET,\Delta S}\mathrm{cov}(PET, \Delta S) \end{aligned} \tag{10}$$

where σ^2 and cov( ) indicate the variance and covariance of different factors, respectively. Additionally, w_i before the different variance (or covariance) terms represents the corresponding weighting factors, respectively, which can effectively quantify the contributions of different factors to R variance and can be analytically estimated from the long-term average aridity index ($\bar{\varnothing} = \overline{PET}/\bar{P}$) in combination with the Budyko framework. Different weighting factors are presented as follows:

$$w_P = [1 - F(\bar{\varnothing}) + F'(\bar{\varnothing})\bar{\varnothing}]^2 \tag{11}$$

$$w_{\Delta S} = [1 - F(\bar{\varnothing}) + F'(\bar{\varnothing})\bar{\varnothing}]^2 \tag{12}$$

$$w_{PET} = [F'(\bar{\varnothing})]^2 \tag{13}$$

$$w_{P,PET} = -2[1 - F(\bar{\varnothing}) + F'(\bar{\varnothing})\bar{\varnothing}]F'(\bar{\varnothing}) \tag{14}$$

$$w_{P,\Delta S} = -2[1 - F(\bar{\varnothing}) + F'(\bar{\varnothing})\bar{\varnothing}]^2 \tag{15}$$

$$w_{PET,\Delta S} = 2[1 - F(\bar{\varnothing}) + F'(\bar{\varnothing})\bar{\varnothing}]F'(\bar{\varnothing}) \tag{16}$$

where $\bar{\varnothing}$ ($= \overline{PET}/\bar{P}$) is the long-time average aridity index; $F(\bar{\varnothing})$ and $F'(\bar{\varnothing})$ represent the original Budyko framework and its first-order derivative, respectively; and w_i refers to different weighting factors. In these equations, a positive (or negative) weighting factor indicates that an increase (or decrease) in the corresponding term (such as σ_P^2, σ_R^2 and $\sigma_{\Delta S}^2$) will result in an increase (decrease) in runoff variance (σ_R^2). For example, if w_p is equal to 0.1, this means that a 10% increase of precipitation variance (σ_P^2) would simultaneously bring a 1% increase in runoff variance (σ_R^2). According to Equations (10) and (11)–(16), runoff variance across the SRYR can be finally partitioned into variances from climatic variables and basin storage including P, PET and ΔS.

RESULTS

Monthly time series of *P*, *PET*, *ET* and *R* during 2003–2014

Figure 2 presents the monthly time series of P, PET, ET and R during the study period across the selected SRYR. It has been challenging to acquire accurate *in situ* measurements of actual ET for large basins such as the SRYR with few meteorological and hydrological observations. As shown in Figure 2, the mean monthly ET across the SRYR ranges from 11.5 to 88.2 mm during 2003–2014. In addition,

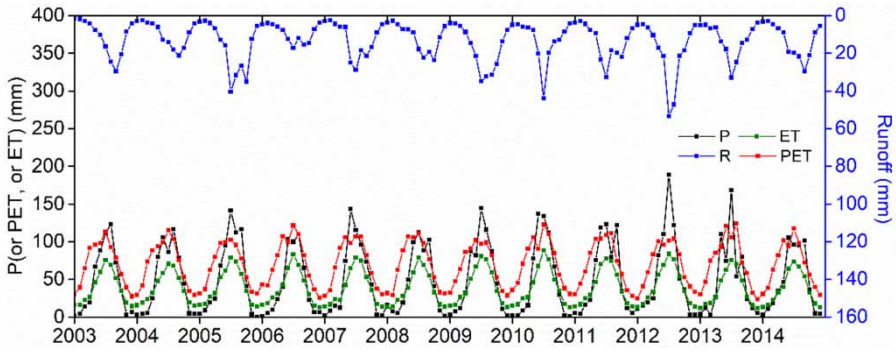

Figure 2 | Comparisons between monthly time series of precipitation (*P*), potential evapotranspiration (*PET*), evapotranspiration (*ET*) and runoff (*R*) during 2003–2014 across the SRYR. The correlation coefficients (*r*) between *R* and *P*, *PET*, *ET* are $r = 0.79$, $r = 0.54$ and $r = 0.78$, respectively.

monthly *PET* shows distinct seasonal variations with a wide span from 23.5 to 123.8 mm. Mean monthly precipitation has a wide range from 0.3 to 188.5 mm. Generally, it shows an obvious seasonal cycle with a maximum value in summer (June to August) and a minimum value in winter (December to February), which is in line with the results from previous studies (Meng *et al.* 2014; Deng *et al.* 2020). Monthly time series of runoff is also acquired from the TNH station, which shows a reasonable correspondence with the precipitation and *ET* shown in Figure 2.

Validation of changes in terrestrial water storage across the SRYR

To better understand the variations of water cycles and their response to climatic variability across the SRYR, the ΔS at different time scales (monthly, seasonal and annual, respectively) is needed. In this study, regional ΔS is estimated as the residual of water balance closure. As shown in Figure 3, monthly time series of ΔS based on the water balance method shows a seasonal variation with a wide range from −41.2 to 59.8 mm.

Since the aforementioned results are directly estimated by the water balance method, it is necessary to further validate monthly time series of ΔS against the GRACE-derived observations across the SRYR. The values of RMSE and correlation coefficient (*r*) are 14.05 mm and 0.79, respectively. Overall, there exists a statistically significant positive correlation at the 0.05 significance level ($p < 0.05$) between ΔS estimated by the water balance method and that derived from GRACE data across the study region, which reach to maximum and minimum values almost simultaneously during 2003–2014. All the results shown in Figure 3 indicate that monthly time series of ΔS based on the water balance

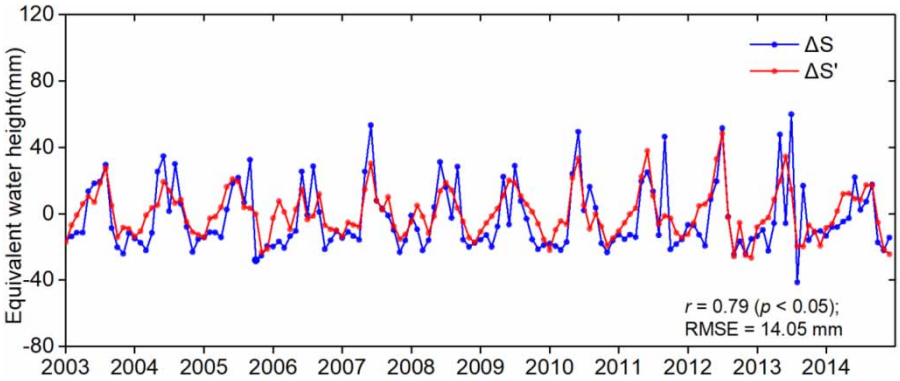

Figure 3 | Monthly time series of changes in terrestrial water storage estimated by the water balance method (ΔS) and derived from GRACE data ($\Delta S'$) during 2003–2014 across the SRYR.

method are reasonable and acceptable for the SRYR. Furthermore, estimated monthly ΔS can be added into annual and seasonal time series of ΔS, respectively.

Effect of ΔS on water balance at different time scales

Monthly scales

The Budyko curves for the monthly datasets across the SRYR during 2003–2014 have been shown in Figure 4. *ET* and *PET* for regions are scaled by *P* and *P*′, respectively, with the goal of illustrating the importance and necessity of considering ΔS when applying the Budyko framework to assess runoff variance over a time interval. Due to the influence of ΔS on hydrological cycles, there exist significant differences between Figure 4(a) and 4(b). As shown in Figure 4(a), the evapotranspiration ratio (*ET*/*P*) increases linearly with the increasing aridity index (*PET*/*P*) when neglecting the effects of ΔS at the monthly scale. In addition, many data points of *PET*/*P* and *ET*/*P* obviously depart from the theoretical Budyko curve, and some scatter points even fall above the water limit line of Budyko space (i.e. $ET/P > 1$). This is inconsistent with the previous results found by Chen *et al.* (2020), who stated that the obvious linear relationship between *ET*/*P* and *PET*/*P* can be captured at the monthly scale in some typical arid and semi-arid regions.

In contrast, the data points of *PET*/*P*′ and *E*/*P*′ considering ΔS generally follow the theoretical Budyko curve well when considering ΔS for the SRYR at the monthly scale as shown in Figure 4(b). Overall, the points scaled by *P*′ (i.e. with considering ΔS, Figure 4(b)) are denser than those scaled by *P* (i.e. without considering ΔS, Figure 4(a)) at the monthly scale. Additionally, the data points considering ΔS ($R^2 = 0.49$) show a better performance in the fitting of Budyko curves than those without considering ΔS ($R^2 = 0.11$), indicating that ΔS plays an important role in the basin-scale water and energy balance. The above results further reflect that regional ΔS indeed makes up a large proportion of the partitioning of *P* into *R* (or *E*), and therefore it should be taken into consideration when analyzing the hydrological cycles at the monthly scale.

Seasonal scales

Investigating the water and energy budget over regions at seasonal scales can help us better understand the variability in runoff, which is important and meaningful for predicting some extreme events such as droughts or floods in advance under climatic variability, especially in some ungauged basins. Therefore, the Budyko framework is also applied in the SRYR using seasonal time series of data during the study period. Similar to the results shown in Figure 4, Figure 5 also presents the water balance in the Budyko curve for the SRYR. The results in Figure 5(a) demonstrate that the data points representing *PET*/*P* versus E/P distribute as linear curves rather than the Budyko curves as expected while assuming that ΔS was negligible at the seasonal scale. Some data points exceeded the 'water limit' boundary represented by $ET/P = 1$ in Figure 5(a), indicating that actual *ET* is more than the amount of *P* due to the neglect of ΔS in the water balance equation.

Figure 5(b) presents the ratio of seasonal actual evapotranspiration to available precipitation (*ET*/*P*′) as a function of corresponding dryness index (*PET*/*P*′)

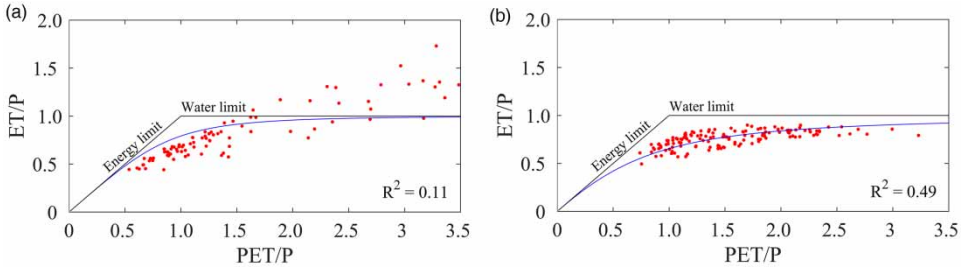

Figure 4 | Budyko curves across the SRYR at the monthly scale. Red points denote (a) *PET*/*P* versus *ET*/*P* (without considering ΔS) and (b) *PET*/*P*′ versus *ET*/*P*′ (considering ΔS), respectively. Please refer to the online version of this paper to see this figure in colour: http://dx.doi.org/10.2166/nh.2021.179.

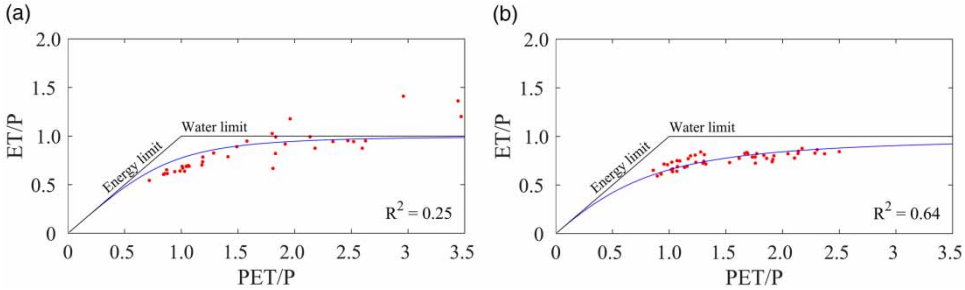

Figure 5 | Budyko curves across the SRYR at the seasonal scale. Red points denote (a) *PET/P* versus *ET/P* (without considering ΔS) and (b) *PET/P′* versus *ET/P′* (considering ΔS), respectively. Please refer to the online version of this paper to see this figure in colour: http://dx.doi.org/10.2166/nh.2021.179.

considering ΔS for the SRYR. As expected, the data points considering ΔS in the study period present a perfect Budyko relationship at the seasonal time scale as depicted in Figure 5(b). In other words, the extended Budyko framework considering ΔS (i.e. Equation (6)) can accurately capture the seasonal variability of the regional water and energy balance across the SRYR in this figure.

Annual scales

At the annual scale, both the scatter points shown in Figure 6(a) and 6(b) follow an approximate Budyko-like distribution as expected, with none of them falling in the region limited by water and energy boundary. Furthermore, it can be found that most of the data points are well located in the nearby region of the theoretical Budyko curve except one point shown in Figure 6(a), which may be caused by the neglect of ΔS.

Figure 6(b) shows the corresponding extended Budyko framework for the annual datasets across the study region during the study period. The results shown in Figure 6(b) show that all data points representing *PET/P′* versus *ET/P′* distribute in the regions of theoretical Budyko curve perfectly. Namely, the balance between water availability and energy supply at the annual scale for the SRYR can be explained well by the extended Budyko relationship. This finding is highly in line with Yang *et al.* (2007) who stated that this extended Fu's equation can be used for predicting the inter-annual variability of regional water balances.

In general, using the newly modified effective precipitation ($P' = P - \Delta S$) as the proxy of total water availability for closed basins, the data points of *PET/P′* and *ET/P′* ($R^2 = 0.81$) generally show a better performance in the fitting of the Budyko relationship than those without considering ΔS ($R^2 = 0.67$). In particular, the original Budyko framework using the precipitation as the available water resource is reasonable and applicable for the long-term hydrological cycles of natural and closed catchments because ΔS is relatively small compared to variations in runoff and the other variables such as P or ET at the

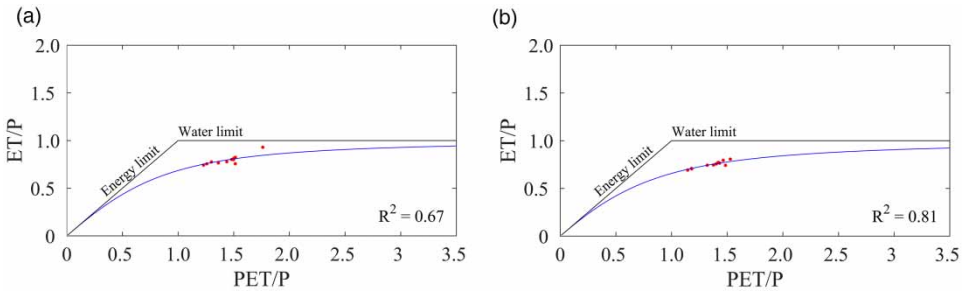

Figure 6 | Budyko curves across the SRYR at the annual scale. Red points denote (a) PET/P versus *ET/P* (without considering ΔS) and (b) *PET/P′* versus *ET/P′* (considering ΔS), respectively. Please refer to the online version of this paper to see this figure in colour: http://dx.doi.org/10.2166/nh.2021.179.

annual scale. When the time scale becomes finer, the contribution of ΔS to the water balance will become bigger, which indicates that the effects of ΔS are generally significant in the SRYR at the monthly and seasonal scale.

Contributions of climate factors and basin storage to runoff variance based on the extended Budyko framework

It is widely known that runoff is closely related to regional water resource management and planning, which is of critical importance for sustainable social and economic development (Mccabe & Wolock 2011; Fowler *et al.* 2016). In fact, variation in runoff is usually viewed as one of the most important indicators that can reflect the true state of regional available water. Therefore, deep insights into runoff variance can help us better assess how regional water availability (in the form of runoff) has changed in the past decade. According to the newly proposed variance decomposition framework (i.e. Equation (10)), a quantitative assessment of the contributions of different factors in hydrological cycles (i.e. P, PET and ΔS) to the variance in runoff at different time scales can be implemented across the SRYR. By incorporating ΔS into the Budyko framework, the critical role of ΔS in water and energy cycle dynamics, especially in runoff variance, has been highlighted. Results of different weighting factors shown in the variance decomposition framework (i.e. Equation (10)) are shown in Figure 7, which represents the corresponding contributions to runoff variance when the same changes occurred in each term. It can be found that the value of w_P is identical to that of $w_{\Delta S}$ shown in Equation (10), which indicates that P and ΔS can make same contributions to runoff variance on the condition that same variations occur in P and ΔS, respectively. Additionally, the negative contribution from the covariance between P and ΔS (i.e. $w_{P,\ \Delta S}$) to runoff variance is the most significant among all weighting factors with a value of -0.43. In comparison with the other weighting factors listed in Figure 7, the contribution of variance in PET (i.e. w_{PET}) to runoff variance is relatively insignificant with a value of $+0.03$.

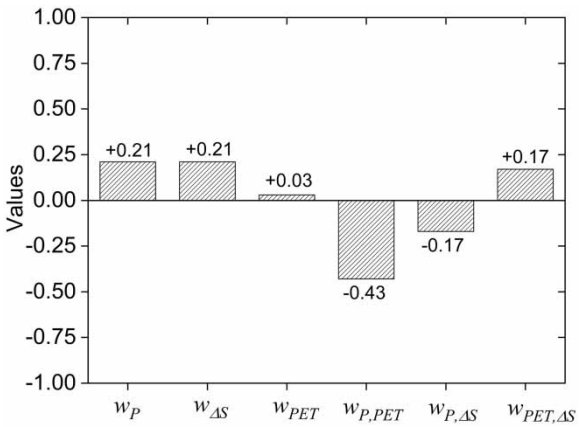

Figure 7 | Results of each weighting factor shown in the variance decomposition framework (Equation (10)). *Note:* '+' refers to a positive contribution to runoff variance; '−' refers to a negative contribution to runoff variance.

The contributions of each variable to runoff variance at different time scales have been depicted in Figure 8. As shown in Figure 8(a), runoff variance at the monthly scale mainly comes from P, while the contribution from PET is relatively small. Notably, ΔS obviously plays an important role in runoff variance when compared to PET, although it has been neglected in previous studies (Jiang *et al.* 2015; Wu *et al.* 2017b; Wang *et al.* 2019). Some other terms in Equation (10), such as $w_{P,PET}\mathrm{cov}(P, PET)$ and $w_{P,PET}\mathrm{cov}(P, \Delta S)$, generally make obviously negative contributions to runoff variance, which indicate that the source of runoff reduction mainly arises from the covariance between P and PET (or ΔS). In addition, variance in runoff estimated by Equation (10) (σ_R^2_sim) has a good agreement with that derived from observations (σ_R^2_obs) at the monthly scale with a small bias of 7%, which demonstrates that the variance decomposition framework is applicable and effective to assess the contributions of terms to runoff variance across the SRYR.

The contributions of different factors to variance in runoff at the seasonal scale show a similar pattern to that at the monthly scale after comparing Figure 8(a) and 8(b). As shown in Figure 8(b), P is still the most important source that results in the variations in runoff. At the same time, both ΔS and PET also have positive effects on runoff variance. In contrast, the negative contribution to the runoff variance results from the terms, including $w_{P,PET}\mathrm{cov}(P, PET)$ and $w_{P,PET}\mathrm{cov}(P, \Delta S)$, which is similar to that shown in Figure 8(a). Additionally, variance in runoff predicted by Equation (10) (σ_R^2_sim) is 847 mm^2, which is rather close to the results derived from observations (σ_R^2_obs) at the seasonal scale (i.e. 736 mm^2) with a relative bias of 15%.

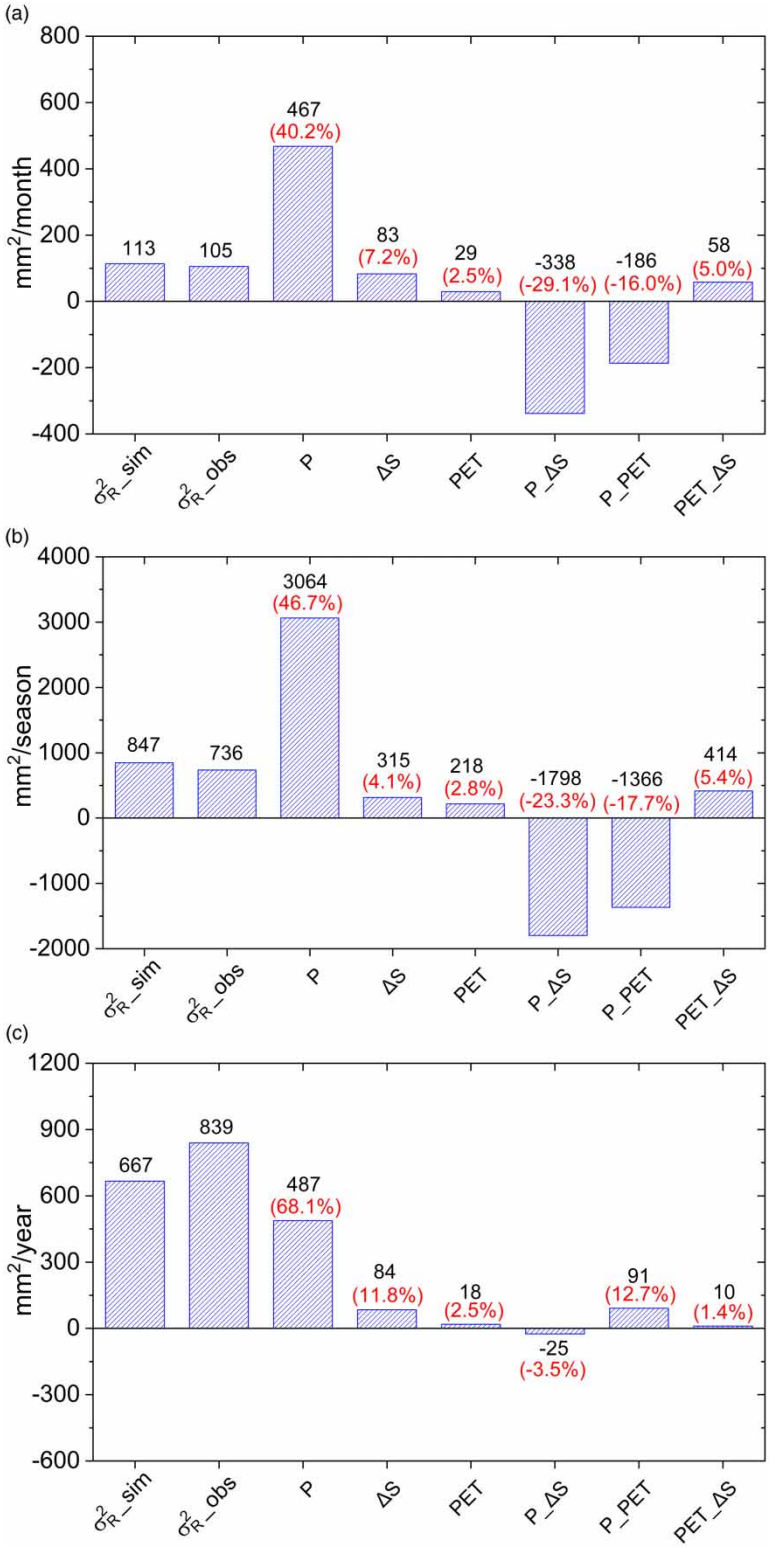

Figure 8 | Contributions of climate factors (*P* and *PET*) and basin storage (Δ*S*) to runoff variance across the SRYR at (a) monthly scale, (b) seasonal scale and (c) annual scale, respectively. Note that the scales of *y*-axis in different subfigures are not always the same.

The contributions of different climate factors and basin storage to runoff variance at the annual scale are also plotted in Figure 8(c). Undoubtedly, P, as a considerably remarkable impact factor, greatly affects runoff variance at the annual scale. ΔS is another critical contributing factor in enhancing the inter-annual variance in runoff. Notably, it can be observed from Figure 8(c) that the contribution of ΔS to runoff variance is more significant at the monthly scale than that at the annual scale because ΔS is more sensitive to the monthly climatic fluctuation than annual fluctuation. In addition, the terms of covariance between P and ΔS have a negative contribution to variance in runoff. The contributions of other terms to inter-annual runoff variance also have been shown in Figure 8(c), respectively.

According to the proposed variance decomposition framework, the contributions of different climate factors and basin storage to runoff variance for the SRYR have been fully quantified. Overall, P contributes more to runoff variance than the other factors such as PET and ΔS because it is the most important input for regional water balance. Especially, this study emphasizes the effect of ΔS on runoff variance. As mentioned in Figure 8, the effects of ΔS on runoff variance mainly come from three parts, that is, ΔS and the related covariance terms including $w_{P,PET}\mathrm{cov}(P, PET)$ and $w_{P,PET}\mathrm{cov}(P, \Delta S)$. It should be noted that ΔS can contribute more to the variance in runoff than PET. Although the effects of ΔS have long been neglected in previous studies (Jiang *et al.* 2015; Wang *et al.* 2019), the results from this study have demonstrated that ΔS may play a critical role in runoff variance. Obviously, the runoff variance simulated by Equation (10) would be possibly underestimated or overestimated at any time scales without considering the effect of ΔS.

DISCUSSION

Performance of Budyko framework at different time scales

To investigate the role of ΔS (including variations in surface water storage, soil moisture storage and groundwater storage) in the water balance of the SRYR, the variation in terrestrial water storage has been firstly estimated, which shows good agreement with that derived from GRACE data. ΔS and other factors including P and PET were jointly used to analyze the regional water and energy balance at different time scales based on the Budyko framework as mentioned in the 'Results' section.

Overall, the results demonstrate that it is reasonable to exclude the variations in terrestrial water storage from precipitation (i.e. $P' = P - \Delta S$), which is more consistent with the water availability concept in boundary conditions of the original Budyko framework, especially at finer time scales such as monthly or seasonal (Chen *et al.* 2020). Meanwhile, this result repeatedly shows the importance of ΔS when analyzing the regional water balance, since the water available estimation by using P only is highly overestimated. Similar results also have been obtained in some other regions around the world (Zeng & Cai 2016).

Main factors controlling runoff variance at different time scales

The variance decomposition framework of the runoff was applied at monthly, seasonal and annual scales independently. The results show that the runoff variance simulated by the decomposition framework is in line with that observed by the hydrological station in general. However, there still exists some discrepancy between the simulated runoff variance and that derived from observations, especially at the annual scale. This phenomenon can be explained by the following two factors. On one hand, precipitation is viewed as the sole water input for hydrological cycles in the study region when estimating ΔS based on the water balance method, which has proved to be reliable and robust across the SRYR. However, some other natural water resources, such as the melting of snow or glaciers, are not taken into consideration due to the lack of *in situ* observations. On the other hand, the term of aridity index (i.e. $\bar{\varnothing}$) in Equations (11)–(16) is supposed to reflect the long-term mean climate condition for the SRYR while the annual sample data in this study are relatively limited, which is an important reason why the estimated runoff variance is considerably lower than the observations at the annual scale when applying the decomposition framework. The decomposition framework proposed in this study can be better validated on the

condition that more observations about ΔS at the annual scale are available.

Uncertainties and limitations

In this study, different terms in the water balance method are realistically derived from the meteorological stations. In fact, it remains a big challenge to obtain accurate and reliable estimations about precipitation or *PET* in high-altitude regions such as the SRYR. Furthermore, extremely limited meteorological stations also make it more difficult to capture the true state of water and energy balance cycles in this region. *ET*, as one of the most difficult variables to obtain or measure, at regional and basin scales, is difficult to be accurately estimated due to its link to Earth's water, energy and carbon cycles (Wang *et al.* 2018). Therefore, the average of three widely used *ET* products is adopted to describe the variations in *ET* with the goal of reducing error and uncertainty. However, the uncertainty of different terms mentioned above will further lead to an error in ΔS through the water balance method (i.e. Equation (2)) via the principle of uncertainty propagation. As documented in previous studies (Rodell *et al.* 2004b; Xie *et al.* 2019a), ΔS estimated by the water balance method is vulnerable to input uncertainty induced by different terms as mentioned above. Although the observations derived from the GRACE satellite can further help us validate the accuracy and reliability of ΔS estimated by the water balance method to some extent, it still inevitably leads to some errors or uncertainties in the estimation of ΔS for the SRYR due to its complicated geophysical conditions and extremely limited observations. In other words, the input uncertainty of Equation (10) may be an important reason why different data points (ET/P versus PET/P or ET/P' versus PET/P') are not fully fitted with the Budyko curve.

The newly proposed variance decomposition framework is physically robust, while some high-order terms in this equation have been neglected in this study for simplicity. Although the errors induced by these high-order terms are relatively limited, it may still lead to some discrepancies between the estimated and theoretical results. Given the above reasons, runoff variance estimated by the proposed variance decomposition framework would be possibly overestimated or underestimated. Therefore, more efforts will be made in our next study to reduce these errors and obtain more reliable results.

CONCLUSIONS

This study applied the original and extended Budyko framework to investigate the role of ΔS in water and energy balance across the SRYR at different time scales. A new variance decomposition framework was also proposed to partition the variance in runoff into different climate factors and basin storage. The major findings from this study are summarized as follows:

(1) Variations in terrestrial water storage have proved to play an important role in the hydrological cycles, and neglecting the effects of ΔS would result in obvious errors when applying the original Budyko framework to analyze the water and energy balance for regions, especially at fine time scales such as month or season. In comparison with the original Budyko framework, the extended Budyko framework considering ΔS can better reflect the true process of exchange between water and energy across the study region.

(2) The variance decomposition framework proposed in this study can be applied to effectively assess the contributions of different climatic factors and basin storage to the variance in runoff at different time scales. It was found that this method is more effective at monthly or seasonal scales than at the annual scale, which may result from the limitation of sample data available at annual scales.

(3) According to the proposed variance decomposition framework, P is the main source of the variance in runoff for the SRYR and has significantly positive effects on variance in runoff. ΔS makes a positive contribution to variance in runoff, which is more significant at monthly and seasonal scales than the annual scale. In addition, the different covariance terms between P and PET (or ΔS) can have a significant influence on variance in runoff.

The conclusions drawn from this study may help us better understand the response of hydrologic cycles under

climatic variability across the SRYR, which can provide valuable guidance for decision-makers in evaluating and predicting water resources. According to the extended Budyko framework, the variance decomposition framework proposed in this study can make a quantitative assessment of the influence of climatic variability on runoff changes, which can be applied in other study regions.

ACKNOWLEDGEMENTS

We sincerely thank the NASA MEaSUREs Program for providing GRACE-JPL mascon solutions and the Goddard Space Flight Center for providing GSFC mascon solutions. The GRACE-CSR RL05 mascon solutions are provided by the Center for Space Research at the University of Texas at Austin. We thank the Yellow River Conservancy Commission of the Ministry of Water Resources for providing the runoff observations used in this study.

AUTHOR CONTRIBUTIONS

Y.-P.X. and J.X. designed the study; J.X. did the main calculations and wrote the draft of the manuscript; Y.-P.X. guided the research and revised the manuscript; Y.W. and Y.G. performed data preprocessing.

CONFLICT OF INTEREST

The authors declare that they have no known competing financial interests or personal relationships that could have appeared to influence the work reported in this paper.

FUNDING

This work was financially supported by the National Key Research and Development Program of China (Grant No. 2018YFC0407401) and the National Natural Science Foundation of China (Grant No. 52009121).

DATA AVAILABILITY STATEMENT

All relevant data are included in the paper or its Supplementary Information.

REFERENCES

Ahlstrom, A., Canadell, J. G., Schurgers, G., Wu, M., Berry, J. A., Guan, K. & Jackson, R. B. 2017 Hydrologic resilience and Amazon productivity. *Nat. Commun.* **8** (1), 387–387.

Asoka, A., Gleeson, T., Wada, Y. & Mishra, V. 2017 Relative contribution of monsoon precipitation and pumping to changes in groundwater storage in India. *Nat. Geosci.* **10** (2), 109–117.

Awange, J. L., Fleming, K. M., Kuhn, M., Featherstone, W. E., Heck, B. & Anjasmara, I. 2011 On the suitability of the $4^\circ \times 4^\circ$ GRACE mascon solutions for remote sensing Australian hydrology. *Remote Sens. Environ.* **115** (3), 864–875.

Berghuijs, W. R., Larsen, J. R., Van Emmerik, T. H. M. & Woods, R. A. 2017 A global assessment of runoff sensitivity to changes in precipitation, potential evaporation, and other factors. *Water Resour. Res.* **53** (10), 8475–8486.

Bock, A. R., Farmer, W. H. & Hay, L. E. 2018 Quantifying uncertainty in simulated streamflow and runoff from a continental-scale monthly water balance model. *Adv. Water Resour.* **122**, 166–175.

Budyko, M. I. 1974 *Climate and Life*. Elsevier, New York.

Carmona, A. M., Sivapalan, M., Yaeger, M. A. & Poveda, G. 2014 Regional patterns of interannual variability of catchment water balances across the continental U.S.: a Budyko framework. *Water Resour. Res.* **50** (12), 9177–9193.

Chang, Y., Qin, D., Ding, Y., Zhao, Q. & Zhang, S. 2018 A modified MOD16 algorithm to estimate evapotranspiration over alpine meadow on the Tibetan Plateau, China. *J. Hydrol.* **561**, 16–30.

Chen, X., Alimohammadi, N. & Wang, D. 2013 Modeling interannual variability of seasonal evaporation and storage change based on the extended Budyko framework. *Water Resour. Res.* **49**, 6067–6078.

Chen, H., Huo, Z., Zhang, L. & White, I. 2020 New perspective about application of extended Budyko formula in arid irrigation district with shallow groundwater. *J. Hydrol.* **582**, 124496.

Chiew, F. H., Peel, M. C., McMahon, T. A. & Siriwardena, L. W. 2006 *Precipitation Elasticity of Streamflow in Catchments Across the World* (S. Demuth, A. Gustard, E. Planos, F. Scatena, & E. Servat, eds). IAHS Publication, Wallingford, pp. 256–262.

Chu, H., Wei, J., Qiu, J., Li, Q. & Wang, G. 2019 Identification of the impact of climate change and human activities on rainfall-runoff relationship variation in the Three-River Headwaters region. *Ecol. Indic.* **106**, 105516.

Collins, D. N., Davenport, J. L. & Stoffel, M. 2013 Climatic variation and runoff from partially-glacierised Himalayan

tributary basins of the Ganges. *Sci. Total Environ.* **468–469**, 48–59.

Darvini, G. & Memmola, F. 2020 Assessment of the impact of climate variability and human activities on the runoff in five catchments of the Adriatic Coast of south-central Italy. *J. Hydrol.* **31**, 100712.

Deng, X., Song, C., Liu, K., Ke, L., Zhang, W., Ma, R., Zhu, J. & Wu, Q. 2020 Remote sensing estimation of catchment-scale reservoir water impoundment in the upper Yellow River and implications for river discharge alteration. *J. Hydrol.* **585**, 124791.

Dey, P. & Mishra, A. 2017 Separating the impacts of climate change and human activities on streamflow: a review of methodologies and critical assumptions. *J. Hydrol.* **548**, 278–290.

Fowler, K., Peel, M. C., Western, A. W., Zhang, L. & Peterson, T. J. 2016 Simulating runoff under changing climatic conditions: revisiting an apparent deficiency of conceptual rainfall-runoff models. *Water Resour. Res.* **52** (3), 1820–1846.

Fu, B. P. 1981 On the calculation of the evaporation from land surface. *Sci. Atmos. Sin.* **5** (1), 23–31 [in Chinese].

Greve, P., Burek, P. & Wada, Y. 2020 Using the Budyko framework for calibrating a global hydrological model. *Water Resour. Res. Water* **56**, e2019WR026280.

Guo, X., Tian, L., Wang, L., Yu, W. & Qu, D. 2017 River recharge sources and the partitioning of catchment evapotranspiration fluxes as revealed by stable isotope signals in a typical high-elevation arid catchment. *J. Hydrol.* **549**, 616–630.

Irmak, S. & Mutiibwa, D. 2010 On the dynamics of canopy resistance: generalized linear estimation and relationships with primary micrometeorological variables. *Water Resour. Res.* **46** (8), W08256.

Istanbulluoglu, E., Wang, T. J., Wright, O. M. & Lenters, J. D. 2012 Interpretation of hydrologic trends from a water balance perspective: the role of groundwater storage in the Budyko hypothesis. *Water Resour. Res.* **48**, W00H16.

Jiang, C., Xiong, L., Wang, D., Liu, P., Guo, S. & Xu, C. 2015 Separating the impacts of climate change and human activities on runoff using the Budyko-type equations with time-varying parameters. *J. Hydrol.* **522**, 326–338.

Khan, M. S., Liaqat, U. W., Baik, J. & Choi, M. 2018 Stand-alone uncertainty characterization of GLEAM, GLDAS and MOD16 evapotranspiration products using an extended triple collocation approach. *Agric. For. Meteorol.* **252**, 256–268.

Landerer, F. W. & Swenson, S. C. 2012 Accuracy of scaled GRACE terrestrial water storage estimates. *Water Resour. Res.* **48** (4), W04531.

Lei, H., Yang, D. & Huang, M. 2014 Impacts of climate change and vegetation dynamics on runoff in the mountainous region of the Haihe River basin in the past five decades. *J. Hydrol.* **511**, 786–799.

Leuning, R., Zhang, Y., Rajaud, A., Cleugh, H. A. & Tu, K. P. 2008 A simple surface conductance model to estimate regional evaporation using MODIS leaf area index and the Penman-Monteith equation. *Water Resour. Res.* **44** (10), W10419.

Li, F., Zhang, Y., Xu, Z., Teng, J., Liu, C., Liu, W. & Mpelasoka, F. 2013 The impact of climate change on runoff in the southeastern Tibetan Plateau. *J. Hydrol.* **505**, 188–201.

Li, Z., Shi, X., Tang, Q., Zhang, Y., Gao, H., Pan, X., Dery, S. J. & Zhou, P. 2020 Partitioning the contributions of glacier melt and precipitation to the 1971–2010 runoff increases in a headwater basin of the Tarim River. *J. Hydrol.* **583**, 124579.

Liang, W., Bai, D., Wang, F., Fu, B., Yan, J., Wang, S., Yang, Y., Long, D. & Feng, M. 2014 Quantifying the impacts of climate change and ecological restoration on streamflow changes based on a Budyko hydrological model in China's Loess Plateau. *Water Resour. Res.* **51**, 6500–6519.

Liang, S., Ge, S., Wan, L. & Zhang, J. 2010 Can climate change cause the Yellow River to dry up? *Water Resour. Res.* **46** (2), W02505.

Liu, W., Wang, L., Zhou, J., Li, Y., Sun, F., Fu, G., Li, X. & Sang, Y. 2016 A worldwide evaluation of basin-scale evapotranspiration estimates against the water balance method. *J. Hydrol.* **538**, 82–95.

Long, D., Longuevergne, L. & Scanlon, B. R. 2014 Uncertainty in evapotranspiration from land surface modeling, remote sensing, and GRACE satellites. *Water Resour. Res.* **50** (2), 1131–1151.

Luthcke, S. B., Sabaka, T. J., Loomis, B. D., Arendt, A. A., McCarthy, J. J. & Camp, J. 2013 Antarctica, Greenland and Gulf of Alaska land-ice evolution from an iterated GRACE global mascon solution. *J. Glaciol.* **59** (216), 613–631.

Lv, M., Ma, Z., Yuan, X., Lv, M., Li, M. & Zheng, Z. 2017 Water budget closure based on GRACE measurements and reconstructed evapotranspiration using GLDAS and water use data for two large densely-populated mid-latitude basins. *J. Hydrol.* **547**, 585–599.

Ma, H., Yang, D., Tan, S. K., Gao, B. & Hu, Q. 2010 Impact of climate variability and human activity on streamflow decrease in the Miyun Reservoir catchment. *J. Hydrol.* **389** (3), 317–324.

Mallick, K., Boegh, E., Trebs, I., Alfieri, J. G., Kustas, W. P., Prueger, J. H., Niyogi, D., Das, N. N., Drewry, D. T., Hoffmann, L. & Jarvis, A. 2015 Reintroducing radiometric surface temperature into the Penman-Monteith formulation. *Water Resour. Res.* **51** (8), 6214–6243.

Martens, B., Gonzalez Miralles, D., Lievens, H., Van Der Schalie, R., De Jeu, R. A., Fernández-Prieto, D. & Verhoest, N. 2017 GLEAM v3: satellite-based land evaporation and root-zone soil moisture. *Geosci. Model Dev.* **10** (5), 1903–1925.

McCabe, G. J. & Wolock, D. M. 2011 Independent effects of temperature and precipitation on modeled runoff in the conterminous United States. *Water Resour. Res.* **47** (11), W11522.

Mcjannet, D., Cook, F. J. & Burn, S. 2013 Comparison of techniques for estimating evaporation from an irrigation water storage. *Water Resour. Res.* **49** (3), 1415–1428.

Meng, J., Li, L., Hao, Z., Wang, J. & Shao, Q. 2014 Suitability of TRMM satellite rainfall in driving a distributed hydrological model in the source region of Yellow River. *J. Hydrol.* **509**, 320–332.

Miralles, D. G., Holmes, T. R. H., de Jeu, R. A. M., Gash, J. H., Meesters, A. G. C. A. & Dolman, A. J. 2011 Global land-surface evaporation estimated from satellite-based observations. *Hydrol. Earth Syst. Sci.* **15**, 453–469.

Mu, Q., Heinsch, F. A., Zhao, M. & Running, S. W. 2007 Development of a global evapotranspiration algorithm based on MODIS and global meteorology data. *Remote Sens. Environ.* **111**, 519–536.

Patterson, L. A., Lutz, B. D. & Doyle, M. W. 2013 Climate and direct human contributions to changes in mean annual streamflow in the South Atlantic, USA. *Water Resour. Res.* **49** (11), 7278–7291.

Rodell, M., Houser, P. R., Jambor, U., Gottschalck, J., Mitchell, K., Meng, C., Arsenault, K., Cosgrove, B., Radakovich, J., Bosilovich, M., Entin, J. K., Walker, J. P., Lohmann, D. & Toll, D. 2004a The Global Land Data Assimilation System. *Bull. Am. Meteorol. Soc.* **85** (3), 381–394.

Rodell, M., Famiglietti, J. S., Chen, J., Seneviratne, S. I., Viterbo, P., Holl, S. & Wilson, C. R. 2004b Basin scale estimates of evapotranspiration using GRACE and other observations. *Geophys. Res. Lett.* **31** (20), L20504.

Save, H., Bettadpur, S. & Tapley, B. D. 2016 High-resolution CSR GRACE RL05 mascons. *J. Geophys. Res. Solid Earth.* **121**, 7547–7569.

Si, Y., Li, X., Yin, D., Li, T., Cai, X., Wei, J. & Wang, G. 2019 Revealing the water-energy-food nexus in the Upper Yellow River Basin through multi-objective optimization for reservoir system. *Sci. Total Environ.* **682**, 1–18.

Song, C., Ke, L., Huang, B. & Richards, K. 2015 Can mountain glacier melting explains the GRACE-observed mass loss in the southeast Tibetan Plateau: from a climate perspective? *Glob. Planet Change* **124**, 1–9.

Swenson, S. & Wahr, J. 2006 Post-processing removal of correlated errors in GRACE data. *Geophys. Res. Lett.* **33** (8), L08402.

Tikhamarine, Y., Souag-Gamane, D., Ahmed, A. N., Sammen, S. S. & El-Shafie, A. 2020 Rainfall-runoff modelling using improved machine learning methods: Harris hawks optimizer vs. particle swarm optimization. *J. Hydrol.* **589**, 125133.

Walling, D. E. & Fang, D. 2003 Recent trends in the suspended sediment loads of the world rivers. *Glob. Planet Change* **39**, 111–126.

Wan, Z., Zhang, K., Xue, X., Hong, Z., Hong, Y. & Gourley, J. J. 2015 Water balance-based actual evapotranspiration reconstruction from ground and satellite observations over the conterminous United States. *Water Resour. Res.* **51** (8), 6485–6499.

Wang, D. 2012 Evaluating interannual water storage changes at watersheds in Illinois based on long-term soil moisture and groundwater level data. *Water Resour. Res.* **48** (3), W03502.

Wang, D. & Hejazi, M. 2011 Quantifying the relative contribution of the climate and direct human impacts on mean annual streamflow in the contiguous United States. *Water Resour. Res.* **47**, W00J12.

Wang, T., Istanbulluoglu, E., Lenters, J. & Scott, D. 2009 On the role of groundwater and soil texture in the regional water balance: an investigation of the Nebraska Sand Hills, USA. *Water Resour. Res.* **45**, W10413.

Wang, T., Yang, H., Yang, D., Qin, Y. & Wang, Y. 2018 Quantifying the streamflow response to frozen ground degradation in the source region of the Yellow River within the Budyko framework. *J. Hydrol.* **558**, 301–313.

Wang, F., Duan, K., Fu, S., Gou, F., Liang, W., Yan, J. & Zhang, W. 2019 Partitioning climate and human contributions to changes in mean annual streamflow based on the Budyko complementary relationship in the Loess Plateau, China. *Sci. Total Environ.* **665**, 579–590.

Wu, C., Hu, B. X., Huang, G. & Zhang, H. 2017a Effects of climate and terrestrial storage on temporal variability of actual evapotranspiration. *J. Hydrol.* **549**, 388–403.

Wu, J., Miao, C., Wang, Y., Duan, Q. & Zhang, X. 2017b Contribution analysis of the long-term changes in seasonal runoff on the Loess Plateau, China, using eight Budyko-based methods. *J. Hydrol.* **545**, 263–275.

Xie, J., Xu, Y. P., Gao, C., Xuan, W. & Bai, Z. 2019a Total basin discharge from GRACE and Water balance method for the Yarlung Tsangpo River basin, Southwestern China. *J. Geophys. Res. Atmos.* **124**, 7617–7632.

Xie, J., Xu, Y. P., Wang, Y., Gu, H., Wang, F. & Pan, S. 2019b Influences of climatic variability and human activities on terrestrial water storage variations across the Yellow River basin in the recent decade. *J. Hydrol.* **579**, 124218.

Xing, W., Wang, W., Shao, Q., Yong, B., Liu, C., Feng, X. & Dong, Q. 2018 Estimating monthly evapotranspiration by assimilating remotely sensed water storage data into the extended Budyko framework across different climatic regions. *J. Hydrol.* **567**, 684–695.

Xu, S., Yu, Z., Yang, C., Ji, X. & Zhang, K. 2018 Trends in evapotranspiration and their responses to climate change and vegetation greening over the upper reaches of the Yellow River Basin. *Agric. For. Meteorol.* **263**, 118–129.

Xue, B., Wang, L., Li, X., Yang, K., Chen, D. & Sun, L. 2013 Evaluation of evapotranspiration estimates for two river basins on the Tibetan Plateau by a water balance method. *J. Hydrol.* **492**, 290–297.

Yang, D., Sun, F., Liu, Z., Cong, Z., Ni, G. & Lei, Z. 2007 Analyzing spatial and temporal variability of annual water-energy balance in nonhumid regions of China using the Budyko hypothesis. *Water Resour. Res.* **43** (4), W04426.

Yang, H., Yang, D., Lei, Z. & Sun, F. 2008 New analytical derivation of the mean annual water-energy balance equation. *Water Resour. Res.* **44**, W03410.

Yang, H., Xing, L., Xiong, B., Zhang, Q. & Xu, C. 2020 Separating runoff change by the improved Budyko complementary relationship considering effects of both climate change and human activities on basin characteristics. *J. Hydrol.* **591**, 125330.

Yang, L., Feng, Q., Adamowski, J. F., Alizadeh, M. R., Yin, Z., Wen, X. & Zhu, M. 2021 The role of climate change and vegetation greening on the variation of terrestrial

evapotranspiration in northwest China's Qilian Mountains. *Sci. Total Environ.* **759**, 143532.

Yuan, F., Wang, B., Shi, C., Cui, W., Zhao, C., Liu, Y., Ren, L., Zhang, L., Zhu, Y., Chen, T., Jiang, S. & Yang, X. 2018 Evaluation of hydrological utility of IMERG Final run V05 and TMPA 3b42v7 satellite precipitation products in the Yellow River source region, China. *J. Hydrol.* **567**, 696–711.

Zarghami, M., Abdi, A., Babaeian, I., Hassanzadeh, Y. & Kanani, R. 2011 Impacts of climate change on runoffs in East Azerbaijan Iran. *Global Planet. Change* **78** (3–4), 137–146.

Zeng, R. & Cai, X. 2015 Assessing the temporal variance of evaporation considering climate and catchment storage factors. *Adv. Water Resour.* **79**, 51–60.

Zeng, R. & Cai, X. 2016 Climatic and terrestrial storage control on evaporation temporal variability: analysis of river basins around the world. *Geophys. Res. Lett.* **43**, 185–195.

Zhai, R. & Tao, F. 2017 Contributions of climate change and human activities to runoff change in seven typical catchments across China. *Sci. Total Environ.* **605–606**, 219–229.

Zhang, L., Hickel, K., Dawes, W. R., Chiew, F. H. S., Western, A. W. & Briggs, P. R. 2004 A rational function approach for estimating mean annual evapotranspiration. *Water Resour. Res.* **40**, W02502.

Zhang, L., Potter, N., Hickel, K., Zhang, Y. & Shao, Q. 2008 Water balance modeling over variable time scales based on the Budyko framework-model development and testing. *J. Hydrol.* **360** (1–4), 117–131.

Zhang, X., Dong, Q., Cheng, L. & Xia, J. 2019 A Budyko-based framework for quantifying the impacts of aridity index and other factors on annual runoff. *J. Hydrol.* **579**, 124224.

Zhang, H., Zhang, L., Li, J., An, R. D. & Deng, Y. 2020 Monitoring the spatiotemporal terrestrial water storage changes in the Yarlung Zangbo River Basin by applying the P-LSA and EOF methods to GRACE data. *Sci. Total Environ.* **713**, 136274.

Zheng, H., Zhang, L., Liu, C., Shao, X. & Fukushima, Y. 2007 Changes in stream flow regime in headwater catchments of the Yellow River basin since the 1950s. *Hydrol. Process.* **21** (7), 886–893.

Zheng, H., Zhang, L., Zhu, R., Liu, C., Sato, Y. & Fukushima, Y. 2009 Responses of streamflow to climate and land surface change in the headwaters of the Yellow River Basin. *Water Resour. Res.* **45**, 7.

Zheng, Y., Huang, Y., Zhou, S., Wang, K. & Wang, G. 2018 Effect partition of climate and catchment changes on runoff variation at the headwater region of the Yellow River based on the Budyko complementary relationship. *Sci. Total Environ.* **643**, 1166–1177.

Zhou, S., Yu, B., Zhang, L., Huang, Y., Pan, M. & Wang, G. 2016 A new method to partition climate and catchment effect on the mean annual runoff based on the Budyko complementary relationship. *Water Resour. Res.* **52** (9), 7163–7177.

Zuo, D. P., Xu, Z. X., Wu, W., Zhao, J. & Zhao, F. F. 2014 Identification of streamflow response to climate change and human activities in the Wei River Basin, China. *Water Resour. Manage.* **28** (3), 833–8551.

First received 27 November 2020; accepted in revised form 27 March 2021. Available online 12 April 2021